



# Polymer-based Electrochemical Sensor: Fast, Accurate, and Simple Insulin Diagnostics Tool

Ivana Šišoláková<sup>1,2</sup> · Radka Gorejová<sup>1,2</sup> · Frederika Chovancová<sup>1</sup> · Jana Shepa<sup>1</sup> · Fahanwi Asabuwa Ngwabebhoh<sup>2</sup> · Andrea Straková Fedorková<sup>1</sup> · Petr Sába<sup>2</sup> · Renáta Oriňaková<sup>1,2</sup>

Accepted: 21 April 2023  
© The Author(s) 2023

## Abstract

Study of the use of polymers with higher conductivity like polypyrrole, and polyaniline in the electrochemical insulin sensors can overcome the drawbacks arising from the ongoing use of non-conductive polymer membrane. Conductive polymer membranes maintain the positive properties of polymers, like improved stability, reproducibility, and even increase the current response of the prepared sensor toward insulin oxidation. Three different screen-printed electrodes modified with polyaniline, polypyrrole, or chitosan with electrochemically deposited nickel nanoparticles ensuring insulin oxidation were prepared. The electrode morphology was examined via SEM with EDX analysis. Also, the electroactive surface area and stability were determined by voltammetric methods. Based on the results, the SPCEs modified by polypyrrole and nickel nanoparticles were determined as the most appropriate for the insulin determination. The NiNPs-PPy-SPCE exhibited a linear range (500 nM–5 μM), a low-down limit of detection (38 nM), high sensitivity (3.98 μA/μM), and excellent result from insulin determination in real samples (human blood serum). The results confirmed the high potential of developed sensor for future research focused on detection of insulin via electrochemistry methods in clinical samples.

**Keywords** Polymer membrane · Polyaniline · Polypyrrole · Chitosan · Novel sensors · Insulin determination · Diabetes mellitus · Screen-printed carbon electrode

## Introduction

Insulin is known as an anabolic hormone consisting of two chains connected by disulfide bridges [1]. It adjusts the fat, carbohydrate, and protein metabolism by ensuring the transport of glucose from the blood vessels into cells [2]. Insulin secretion dysfunction or inappropriate insulin action is a common cause of cancer, neurodegenerative diseases, and more widespread disease called diabetes mellitus (DM) [3, 4]. In addition, patients suffering with diabetes also face complications including microvascular complications [5], blindness, and chronic kidney diseases [6].

Currently, the commercially used diagnostics test for DM operates on glucose determination using enzymatic glucose sensors [7]. Unfortunately, these sensors exhibit drawbacks arising from the low stability and high price of used enzymes [8–10]. Therefore, to establish a cheap, selective, sensitive, and simple method for insulin detection is of great significance for its diagnosis and monitoring and the prevention of related complications [11]. There are many laboratory methods for insulin determination like bioassays [12], immunoassays [13], high performance liquid chromatography (HPLC), etc. [14]. The huge shortcomings of above mentioned methods are their low sensitivity, low selectivity, high price, and difficult evaluation, which make their use in everyday clinical practice impossible [12, 13, 15]. Overleaf electrochemical non-enzymatic sensing represents simple and highly sensitive method with low detection limit, ease of use and fast, and low price.

Whereas there are no commercially available sensors for insulin determination, various carbon-based electrodes have been widely tested for electrochemical insulin sensor development [16]. Screen-printed carbon electrode (SPCE)

✉ Radka Gorejová  
radka.gorejova@upjs.sk

<sup>1</sup> Department of Physical Chemistry, Faculty of Science, Pavol Jozef Šafárik University, Moyzesova 11, 040 01 Košice, Slovak Republic

<sup>2</sup> Centre of Polymer Systems, Tomas Bata University in Zlín, Třída Tomáše, Bati 5678, 760 01 Zlín, Czech Republic

represents the most appropriate candidate due to the small size of working electrode (WE) and only small amount of analyte required for the determination (50  $\mu\text{L}$ ) [8, 17, 18]. To improve the catalytic activity toward insulin oxidation, various metals (Co, Cu, Ni, Zn) and metal oxide nanoparticles (CuO, NiO, and ZnO) were deposited on the carbon electrode surface [19, 20]. Above-mentioned modifications are still much more cost-effective in comparison with enzymatic sensors. Based on previous known results, Ni nanoparticles (NiNPs) can be considered one of the most suitable modifications of carbon electrode due to excellent electrical properties, low cost, and catalytic activity in the presence of insulin [21, 22].

The usage of polymer membrane is one of the key parameters that need to be included in the construction of electrochemical insulin sensor [23, 25]. The main role of the polymer membrane is the nanoparticle fixation during electrochemical measurement and prevention of  $\text{Cl}^-$  ion adsorption, which is leading to improved sensors' stability and selectivity. Although the above-mentioned polymers stabilize the nanoparticles on the electrode surface, their low conductivity limits their use. Conductive polymers (CP), such as polypyrrole, polyaniline, or polythiophene, represent ideal candidates for further electrode modification due to their electroactivity [26, 27]. CPs are currently used in various applications including health care or energy storage [28] [29]. Furthermore, nanoparticles are capable of improving the properties of conducting polymers, owing to their nanostructures with the expanded active surface area, which results in increased conductivity, electrochemical activity, and higher electron transporter portability [28]. For example, graphite electrode modified by combination of NiNPs and polypyrrole has been studied as potential candidate for non-enzymatic glucose sensor. The results show the excellent properties of developed electrode like low limit of detection (0.4  $\mu\text{M/l}$ ), high sensitivity (2873  $\mu\text{A/mM}$ ), and wide linear range (1–1000  $\mu\text{M/l}$ ) [30].

Polypyrrole (PPy) is characterized by the combined heterocyclic monomers (pyrroles) [31]. The conductivity of PPy relies upon its oxidation state [32]. However, it has been shown that a film of PPy can be over-oxidized when exposed to the positive potential or higher potentials for a specific time [32–34]. There are various ways of PPy preparation including electrochemical polymerization, enzyme-assisted formation, etc. [35]. PPy has extraordinary properties such as electrocatalytic properties [36], excellent adhesive properties [37], biocompatibility [38], and low cost [31]. Because of these properties, it can be considered a suitable material for medical applications [37, 39].

Polyaniline (PANI) is a conductive polymer consisting of aniline monomers [40]. PANI shows remarkable properties like electrical conductivity [41], electroactivity [42], optical properties, biocompatibility [43], excellent stability,

and straightforward synthesis process [41]. Properties of PANI can be easily improved via electrochemical deposition of metal nanoparticles. For example, electrodeposited gold nanostructures (AuNS) on the polyaniline–poly(3,4-ethylenedioxythiophene) (PANI-PEDOT)-modified indium tin oxide electrode show the excellent enhancement of electrochromic properties [44]. Therefore, it has a wide range of applications as sensors—biosensors or gas sensors [43] or in corrosion protection [41].

Herein, the impact of two conductive polymers (polypyrrole and polyaniline) on the determination of insulin via electrochemistry methods on NiNP-modified SPCEs was analyzed. All the results were compared with the electrochemical insulin determination on non-conducting polymer (chitosan)-modified SPCE. The morphology, electrochemical properties, stability, and selectivity of NiNP-polypyrrole-modified SPCE (NiNPs-PPy-SPCE) and NiNPs-polyaniline-modified SPCE (NiNPs-PANI-SPCE) were studied and compared with NiNPs-chitosan-modified SPCE (NiNPs-CHIT-SPCE) using cyclic using various electrochemical methods. Phosphate-buffered saline (PBS) was used as a blank solution for all electrochemical experiments except the real samples analysis where human blood serum was used as a blank solution.

## Methods

### Instrumentations

Cyclic voltammograms and chronoamperograms were obtained from Metrohm AUTOLAB PGSTAT302N potentiostat/galvanostat (Switzerland), combined with a connector for SPCE system. SPCE type 110 was used for all electrochemical measurements made of carbon counter electrode, Ag/AgCl reference electrode, and various modified carbon electrode as the working electrodes. Ag/AgCl reference electrode was used as a pseudoelectrode without any modification prior to the measurements. All experiments were carried on at atmospheric pressure and laboratory temperature. Morphology and surface composition of the WE were studied by scanning electron microscopy (SEM) CrossBeam system (AURIGA Compact mam) with energy dispersive X-ray (EDX) analysis (Germany).

### SPCE Modification

#### NiNPs-CHIT-SPCE

Medium molecular weight chitosan (Sigma Aldrich, USA, Missouri) was dissolved in a deionized water and 0.1 M  $\text{CH}_3\text{COOH}$  to obtain acidic solution (pH = 3). Ten Microliters of the dissolved chitosan was applied on the WE of

SPCE and dried at laboratory conditions. Thereafter, 40 mM  $\text{Ni}(\text{NO}_3)_2 \cdot 6\text{H}_2\text{O}$  (CentralChem, Slovakia) solution with  $\text{pH}=2$  was used for the electrodeposition of the NiNPs on the SPCE, which was further modified with chitosan.  $\text{pH}$  was adjusted by using 0.5 M HCl (Milan Adamik Laboratory Chemicals, Slovakia). The NiNPs were deposited on the electrode surface via pulsed technique using potentials of  $E = +0.4$  V for 5 s.

### NiNPs-PANI-SPCE

Chemical oxidation polymerization method was used to prepare PANI. Initially, 0.5 mL of monomer aniline was dissolved into 10 mL of distilled water containing 1 M HCl. The prepared solution was stirred for 30 min to produce aniline hydrochloride. Subsequently, an ammonium peroxydisulfate solution of same volume as aniline hydrochloride solution was added, and the mixture was homogenized by a mechanical stirrer for 1 h. The concentration used for the preparation of PANI was 0.1 M aniline hydrochloride and 0.125 M ammonium peroxydisulfate. The solid products were separated using filtration technique, washed with 1 M HCl, rinsing with ethanol and then re-dispersed (1 mg/mL) in water/ethanol (1:1 v/v ratio) solution. Ten microliters of the PANI solution was applied on the carbon WE surface and dried at laboratory conditions, followed by the electrodeposition of the NiNPs on the further PANI-modified SPCE surface by adding 40-mM  $\text{Ni}(\text{NO}_3)_2 \cdot 6\text{H}_2\text{O}$  solution. The electrodeposition of the NiNPs on the SPCE was realized via pulse technique as described above to obtain NiNPs-CHIT-SPCE.

### NiNPs-PPy-SPCE

The preparation of polypyrrole (PPy) followed similar procedure as in the case of PANI described above. However, in the place of aniline, pyrrole was used as the reacting monomer by dissolving in 1 M HCl solution. The same volume of ammonium peroxydisulfate was mixed with the pyrrole solution for polymerization. The mixture contained reactant concentrations of 0.1 M pyrrole and 0.125-M ammonium peroxydisulfate. The colorless solution continuously changed to black as the polymerization process reached completion forming polypyrrole (PPy) solids. The produced PPy black solids were filtered and washed with water and ethanol followed by re-dispersion in water/ethanol solution. PPy solution was applied on the carbon WE surface and dried at laboratory conditions followed by the electrodeposition of NiNPs on the modified SPCE to form NiNPs-PPy-SPCE using the same deposition conditions as in NiNPs-PANI-SPCE and NiNPs-chit-SPCE development.

### Insulin Solution Preparation

To obtain the required insulin concentrations, powdered insulin (Sigma Aldrich, Missouri) was dissolved in PBS containing 0.1 M NaOH. To eliminate the influence of solution aging on electrochemical measurements, all solutions were prepared direct before electrochemical measurements. Electrochemical determination of insulin was studied and compared in three different  $\text{pH}$ s (2, 7.4, and 11).  $\text{pH}$  2 was secured with addition of 0.1 M HCl. To determine insulin in real blood serum samples, powdered insulin was dissolved in human blood serum with 0.1 M NaOH.

## Results and Discussion

### Surface Characterization

#### Scanning Electron Microscopy

The scanning electron microscopy images of the bare SPCE and modified electrodes are displayed in Fig. 1 at the same magnification ( $\times 5000$ ). It is visible that, at the bare SPCE surface (Fig. 1A), there is possibility to see inequalities, and the surface of the SPCE is irregular due to the carbon material, which is WE made of. The EDX analysis of the bare SPCE showed 99.5% of carbon, which exactly corresponds to the assumptions. After the modification of bare electrode using polymers in combination with NiNPs, the geometric surface area of WE considerably increased (Fig. 1B–D) due to the clusters of nanoparticles, which are observed on all modified electrodes. The NiNPs cluster size ranged from  $420 \pm 10$  nm (NiNPs-PPy-SPCE) to  $8.4 \pm 0.4$   $\mu\text{m}$  (NiNPs-CHIT-SPCE) in diameter, which was measured using ImageJ software. As can be seen in Fig. 1B (NiNPs-PPy-SPCE), polypyrrole-formed polymer fibers on the electrode surface, leading to the most rapid increase of WE's active surface area (see section *Active surface area determination*) and the increase in conductivity. Corresponding EDX data obtained from EDX spectra (Fig. 1B, D, F, H) indicated the presence of Ni on all modified SPCEs in amounts of 4.6%, 4.2% (Fig. 1F), and 2.5% for NiNPs-PPy-SPCE (Fig. 1D), NiNPs-PANI-SPCE (Fig. 1F), and NiNPs-CHIT-SPCE (Fig. 1H), respectively.

### Area of Electroactive Surface Calculation

The area of electroactive surface of bare SPCE, NiNPs-CHIT-SPCE, NiNPs-PANI-SPCE, and NiNPs-PPy-SPCE was determined via CV using 5 mM  $\text{K}_3[\text{Fe}(\text{CN})_6]/\text{K}_4[\text{Fe}(\text{CN})_6]$  as a model analyte (Fig. 2). The electroactive surface area of WE is different from geometric area due to the inequalities and other influences present on the surface

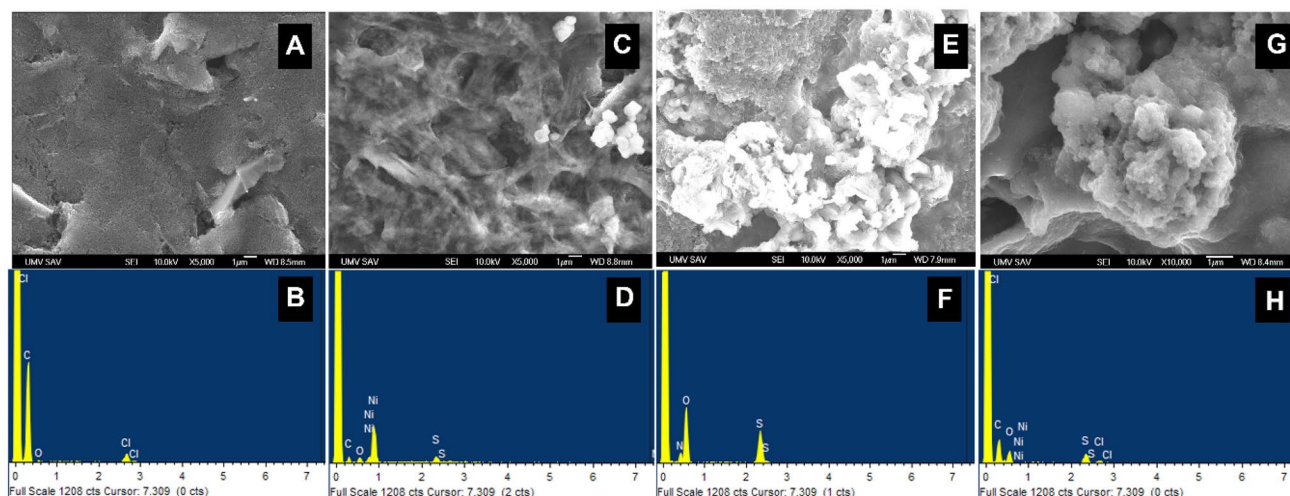


**Fig. 1** SEM micrographs of bare SPCE (A), NiNPs-PPy-SPCE (C), NiNPs-PANI-SPCE (E), and NiNPs-CHIT-SPCE (G) at  $\times 5000$  magnification with EDX spectra of bare SPCE (B), NiNPs-PPy-SPCE (D), NiNPs-PANI-SPCE (F), and NiNPs-CHIT-SPCE (H)

of WEs. The results of this experiment were calculated via Randles–Ševčík equation (Eq. 1) to determine the surface area of WE, which directly participates on the electrochemical processes.

$$I_p = 0.4463nFAc \left( \frac{nFvD}{RT} \right)^{\frac{1}{2}} \quad (1)$$

where  $I_p$  represents the current at anodic peak maximum (A),  $n$  refers to the number of transferred electrons during the electrochemical reaction,  $A$  means active surface area of

WE ( $\text{cm}^2$ ),  $c$  denotes the concentration of the used analyte ( $\text{mol}/\text{cm}^3$ ),  $v$  is the used scan rate ( $\text{V}/\text{s}$ ),  $D$  refers to the diffusion coefficient of used analyte ( $\text{cm}^2/\text{s}$ ),  $R$  is the universal gas constant ( $\text{J}/\text{Kmol}$ ),  $F$  represents the Faraday constant ( $\text{C}/\text{mol}$ ), and  $T$  is the thermodynamic temperature (K).

Figure 2 shows the cyclic voltammogram of the 5 mM  $\text{K}_3[\text{Fe}(\text{CN})_6]/\text{K}_4[\text{Fe}(\text{CN})_6]$  at bare SPCE (violet line), NiNPs-CHIT-SPCE (red line), NiNPs-PANI-SPCE (yellow line), and NiNPs-PPy-SPCE (blue line). As the results show, the current response increased due to the surface modification of the electrode by the conductive polymer in

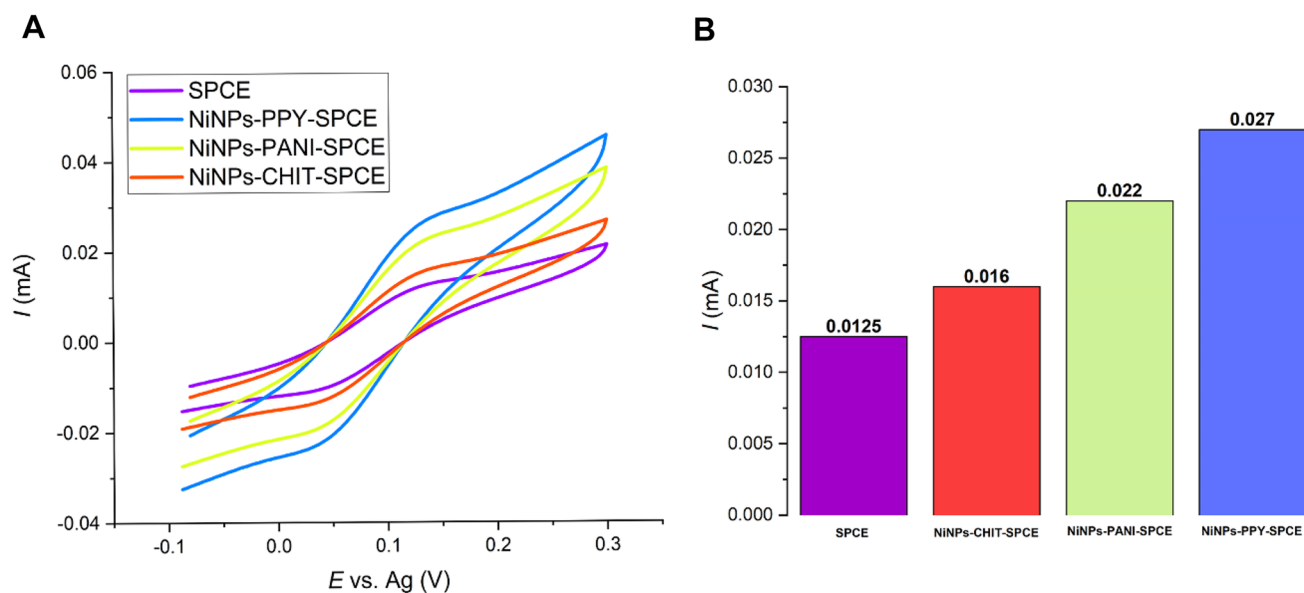
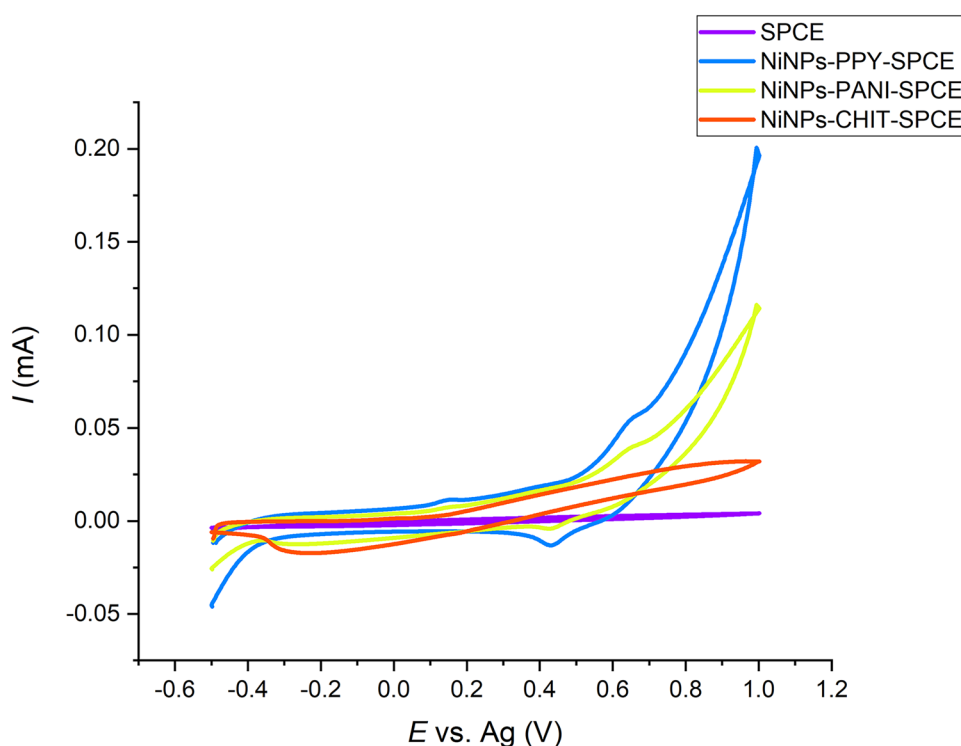


**Fig. 2** Cyclic voltammograms for bare SPCE and different SPCE modifications (A) (SPCE, violet curve; NiNPs-CHIT-SPCE, red curve; NiNPs-PANI-SPCE, green curve; NiNPs-PPy-SPCE, blue

curve) in 5 mM  $\text{K}_3[\text{Fe}(\text{CN})_6]$  in 1 M KCl. Comparison of the maximal current response for each SPCE modification (B)

**Fig. 3** Cyclic voltammograms of 5  $\mu\text{M}$  insulin in 0.1-M NaOH and PBS at bare SPCE (violet line), NiNPs-CHIT-SPCE (red line), NiNPs-PANI-SPCE (yellow line), and NiNPs-PPy-SPCE (blue line)



combination with NiNPs. The calculated area of the electroactive surface of the bare SPCE was determined as 0.016  $\text{cm}^2$ . The electroactive surface of the NiNPs-CHIT-SPCE, NiNPs-PANI-SPCE, and NiNPs-PPy-SPCE was determined as 0.021  $\text{cm}^2$ , 0.038  $\text{cm}^2$ , and 0.046  $\text{cm}^2$ , respectively. The highest area of electroactive surface was determined for NiNPs-PPy-SPCE regarding the extensive active site number created at the WE, which should lead to efficient insulin determination and conductivity increase.

## Electrochemical Measurements

### Comparison of Electrochemical Behavior of Insulin at Bare SPCE, NiNPs-CHIT-SPCE, NiNPs-PANI-SPCE, and NiNPs-PPy-SPCE

To study the electrochemical behavior of bare SPCE, NiNPs-CHIT-SPCE, NiNPs-PANI-SPCE, and NiNPs-PPy-SPCE toward 5  $\mu\text{M}$  insulin in 0.1 mM NaOH and PBS oxidation, CV curves of the above-mentioned SPCEs were obtained. Electrochemical measurements were realized in the following conditions: potential window ranging  $E_1 = +0.5$  V to  $E_2 = +1$  V,  $\nu = 100$  mV/s, number of cycles: 1 (Fig. 3). No current response toward insulin oxidation was registered in the case of bare SPCE (Fig. 3, violet line) due to the absence of catalytically active particles. The highest maximal current value was observed for

NiNPs-PPy-SPCE (Fig. 3, blue line), which led from the significant electroactive surface area increase confirmed by SEM image and calculation of electroactive surface area. The potential ( $E = +0.62$  V) where the maximal current response was recorded appertained to oxidation of insulin on Ni-modified carbon electrode, which further verified the electrocatalytic activity of Ni toward insulin oxidation (see section *Electrochemical determination of insulin on NiNPs-PPY-SPCE and Analytical characteristic calculation*). Insulin oxidation on all modified SPCEs occurs irreversibly due to the difference between cathodic and anodic peak potentials ( $\Delta E = 210$  mV). Taking into account these results and active surface area calculation, NiNPs-PPy-SPCE was used for further analysis as most appropriate for further electrochemical measurements due to its highest conductivity and electrocatalytic activity toward insulin oxidation.

The electrochemical behavior of bare SPCE and modified SPCEs was studied also via EIS. The EIS measurements were realized at the open circuit potential (OCP) within the frequency range from 100 kHz to 0.1 Hz, with the AC magnitude of 10 mV. Measured data were fitted by using Zview software. EIS spectra for different modifications of WE (Fig. 4A) were fitted by equivalent circuits shown in Fig. 4 (B, C). All data are listed in Table 1. The circuit consists of  $R1$ , solution resistance;  $CPE1$ , constant phase element;  $R2$ , charge transfer resistant; and  $Wo1$ , open

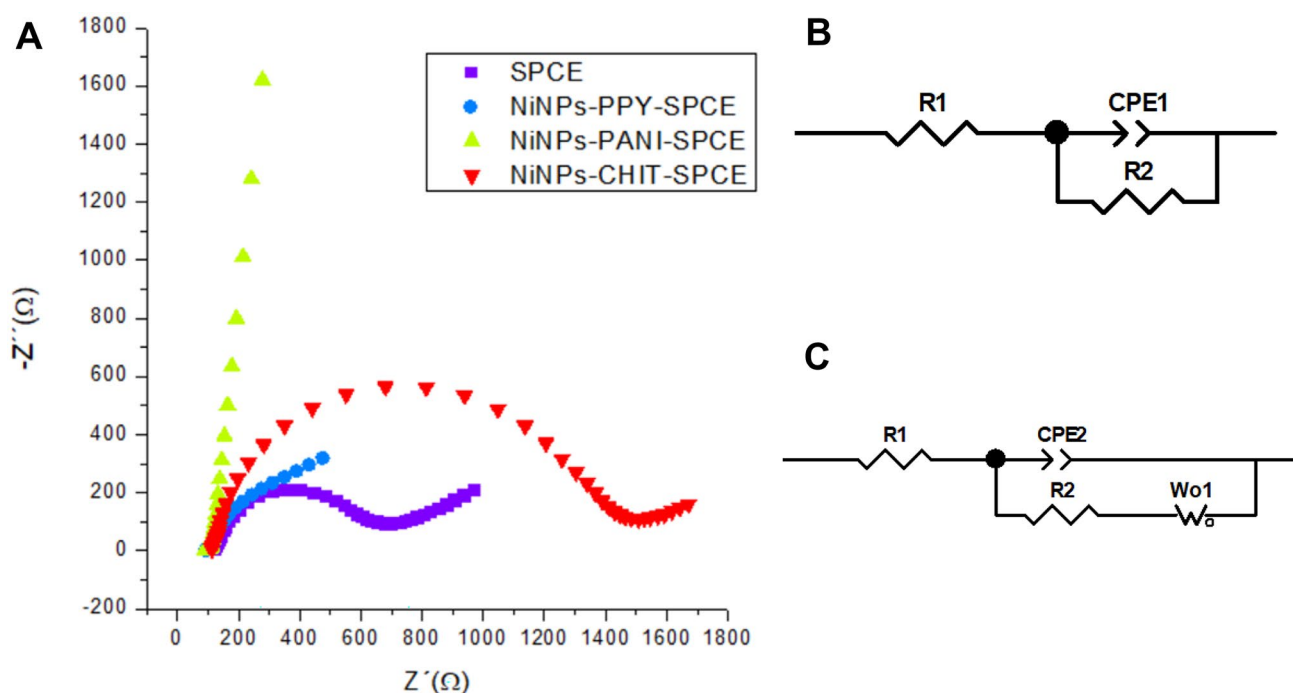


**Fig. 4** (A) Nyquist diagrams obtained at OCP potential (vs. Ag/AgCl pseudoreference electrode) in 5 mM  $K_3[Fe(CN)_6]$  in 1 M KCl at bare SPCE (violet), NiNPs-CHIT-SPCE (red), NiNPs-PANI-SPCE

(yellow), and NiNPs-PPy-SPCE (blue). Equivalent circuit for impedance spectra fitting: NiNPs-PPY-SPCE and NiNPs-PANI-SPCE (B); SPCE and NiNPs-CHIT-SPCE (C)

finite Warburg element. The solution resistance for all electrode modification was approximately the same  $107.7 \Omega \pm 10 \Omega$ . But the charge transfer resistance increased in the order SPCE (479.7  $\Omega$ ), NiNPs-CHIT-SPCE (1269  $\Omega$ ), NiNPs-PPy-SPCE (1286  $\Omega$ ), and NiNPs-PANI-SPCE ( $2.77E+18 \Omega$ ). According to the literature, the order of electrode modification based on charge transfer resistant increase corresponds to the decrease of conductivity of the used polymers [45]. So, the conductivity of prepared electrodes was strongly influenced by used polymer. Double-layer capacitance was also calculated: SPCE (2.90  $\mu\text{F}$ ), NiNPs-PPy-SPCE (6.08  $\mu\text{F}$ ), NiNPs-CHIT-SPCE (1.65  $\mu\text{F}$ ), and NiNPs-PANI-SPCE (248  $\mu\text{F}$ ). The data of the charge transfer resistance and double-layer capacitance corresponds to the result obtained via cyclic voltammetry and corresponds to results in [24, 46]. So, the NiNPs-PPY-SPCE is the most suitable candidate for further determination of insulin.

### Influence of pH on the Electrochemical Determination of Insulin at NiNPs-PPy-SPCE

For the optimization of electrochemical conditions, electrochemical determination of insulin in three different values of pH (2, 7.4, and 11) was studied at NiNPs-PPy-SPCE. As shown in Fig. 5, different pH conditions strongly influenced the shape of CVs. There were no apparent peaks found for the determination of insulin in solution with acidic (Fig. 5, red line) and neutral pH (Fig. 5, green line), confirming that the NiNPs-PPy-SPCE has no catalytic activity in these pHs. The presence of alkaline pH ensures formation of electrocatalytic  $NiO(OH)^-$  species. Mechanism of insulin oxidation at NiNPs-PPy-SPCE surface in alkaline solution can be shown as follows:

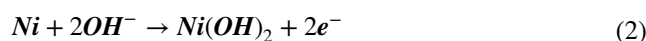
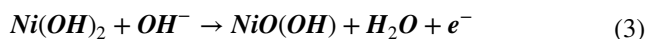
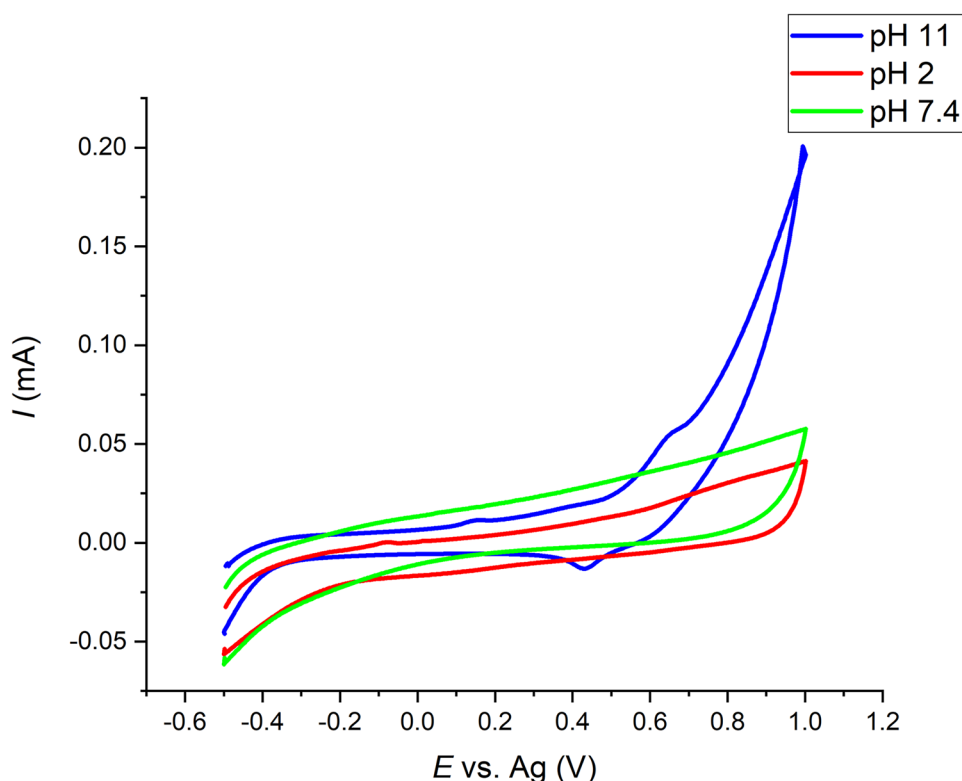


**Table 1** Electrochemical data calculated by fitting EIS spectra to equivalent circuits

Electrode modification	$\chi^2$	RI [ $\Omega$ ]	CPE2-T [ $\mu\text{F}$ ]	CPE2-P [ $\Omega$ ]	Wo1-R [ $\Omega$ ]	Wo1-T [F]	Wo1-P	
SPCE	0.000372	117.8	2.90	0.87	479.7	1059	5759	0.350
NiNPs-PPY-SPCE	0.001647	99.18	6.08	0.71	1286			
NiNPs-PANI-SPCE	0.002441	98.29	248	0.88	$2.77E+18$			
NiNPs-CHIT-SPCE	0.000505	115.7	1.65	0.92	1269	3606	$6.26E-06$	0.196

**Fig. 5** Cyclic voltammograms of 5  $\mu\text{M}$  insulin in PBS (green line) in 0.1 M HCl in PBS (red line) and in 0.1 M NaOH and PBS (blue line) at NiNPs-PPy-SPCE



Due to the obtained results and mechanism of insulin oxidation described above (Eqs. 2–4), it can be assumed that the NiO(OH) particles, which are formed in alkaline pH on NiNPs-PPy-SPCE, represent the active species, which strongly catalyze the direct oxidation of insulin (Eq. 3).

### Stability Test

Stability is one of the most important parameters to be considered for development of suitable electrochemical sensors. Stability tests of the NiNPs-PPy-SPCE after 20 cycles and long-term stability were realized in a 5-mM  $\text{K}_3[\text{Fe}(\text{CN})_6]$ /5 mM  $\text{K}_4[\text{Fe}(\text{CN})_6]$  solution via cycling voltammetry method. A decrease of 11.5% of the maximum current value attributed to the oxidation of  $\text{K}_3[\text{Fe}(\text{CN})_6]$  after 20 cycles is observed in Fig. 6A. Cyclic voltammogram shows that the current decrease after 6 cycles was only 4.1%, which means that the NiNPs-PPy-SPCE can be repeatedly used (maximum 6). Long-term stability results are shown in Fig. 6B, where the maximum current value attributed to the oxidation of  $\text{K}_3[\text{Fe}(\text{CN})_6]$  decrease after 1 week and

1 month was studied. NiNPs-PPy-SPCEs were stored in a dark place without access to light at laboratory temperature ( $t=21^\circ\text{C}$ ). The decrease of maximum current value of 1.4% and 5% was observed after 1 week and 1 month, respectively. Declared results confirmed that the NiNPs-PPy-SPCE is stable after 1 month without significant deterioration of detection properties.

### Direct Electrochemical Insulin Determination on NiNPs-PPy-SPCE and Analytical Characteristic Calculation

The electroanalytical properties of NiNPs-PPy-SPCE were examined via CV (Fig. 7) and CE (Fig. 8) in a solution containing insulin dissolved in 0.1-M NaOH, PBS (pH=11). All electrochemical measurements were performed three times, and average value of the current response together with standard error was included in the dependence of the maximal current value according to insulin oxidation on its concentration (Fig. 7B). Cyclic voltammetry measurements were realized in a potential range applied, which was  $E_1 = +0.2\text{ V}$  and  $E_2 = +1\text{ V}$  with a scan rate of 50 mV/s. Figure 7A shows the cyclic voltammograms of insulin solution with various concentrations (0.5 to 5  $\mu\text{M}$ ) on NiNPs-PPy-SPCE. The peak current corresponding to insulin oxidation on NiNPs-PPy-SPCE ( $E = 0.62\text{ V}$ ) increases linearly

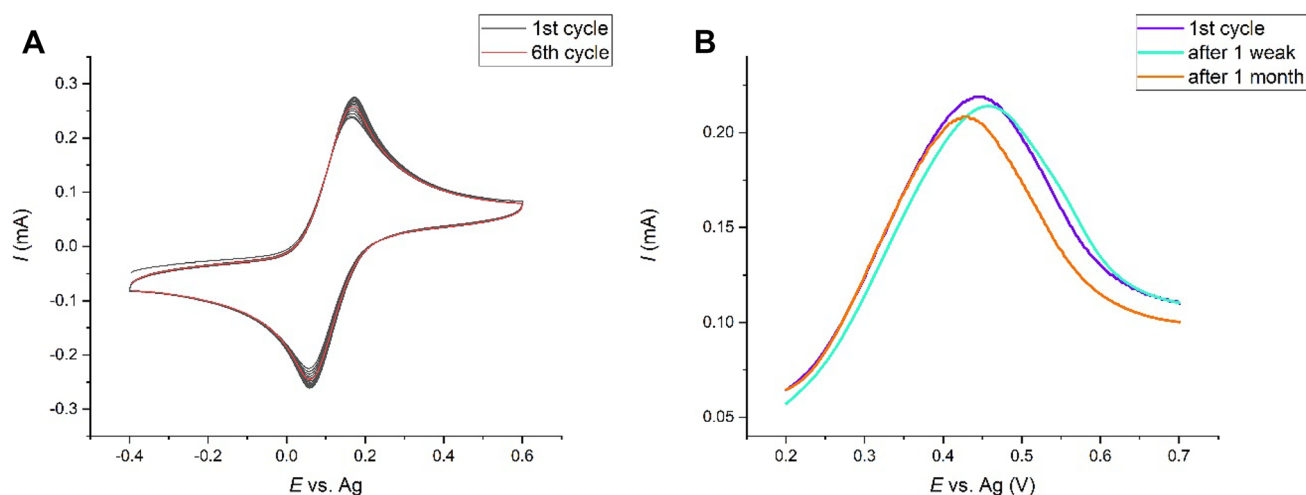


**Fig. 6** The part of cyclic voltammograms of 1-mM  $K_3[Fe(CN)_6]/K_4[Fe(CN)_6]$  on the NiNPs-PPy-SPCE (A) displays the stability of NiNPs-PPy-SPCE after 20 measurement cycles. The part of cyclic

voltammograms of 1-mM  $K_3[Fe(CN)_6]/K_4[Fe(CN)_6]$  on the NiNPs-PPy-SPCE (B) displays the part of first (blue line) cycle and part of cycle obtained after 1 week (turquoise line) and 1 month (red line)

with increasing insulin concentration, as shown in Fig. 7. These results were fitted by linear function (Fig. 7B) to obtain correlation coefficient  $R^2$ -characterized linearity of the given dependency and calculate the sensing characteristics of the NiNPs-PPy-SPCE. This electrode displays following analytical characteristics: linear range, 0.5 to 5  $\mu\text{M}$ , sensitivity of 6.65  $\mu\text{A}/\mu\text{M}$ , and limit of detection (LOD) (0.90 nM). The LOD was calculated from linear regression using the equation below (Eq. 5):

$$LOD = \frac{3 \cdot S_a}{b} \quad (5)$$

where  $S_a$  denotes the standard deviation of the response and  $b$  is the slope of the calibration curve.

Additionally, chronoamperometry as a more sensitive method was used for calculation of electroanalytical characteristics and compared those obtained via CV. The current response exhibited the same trend as in the CV

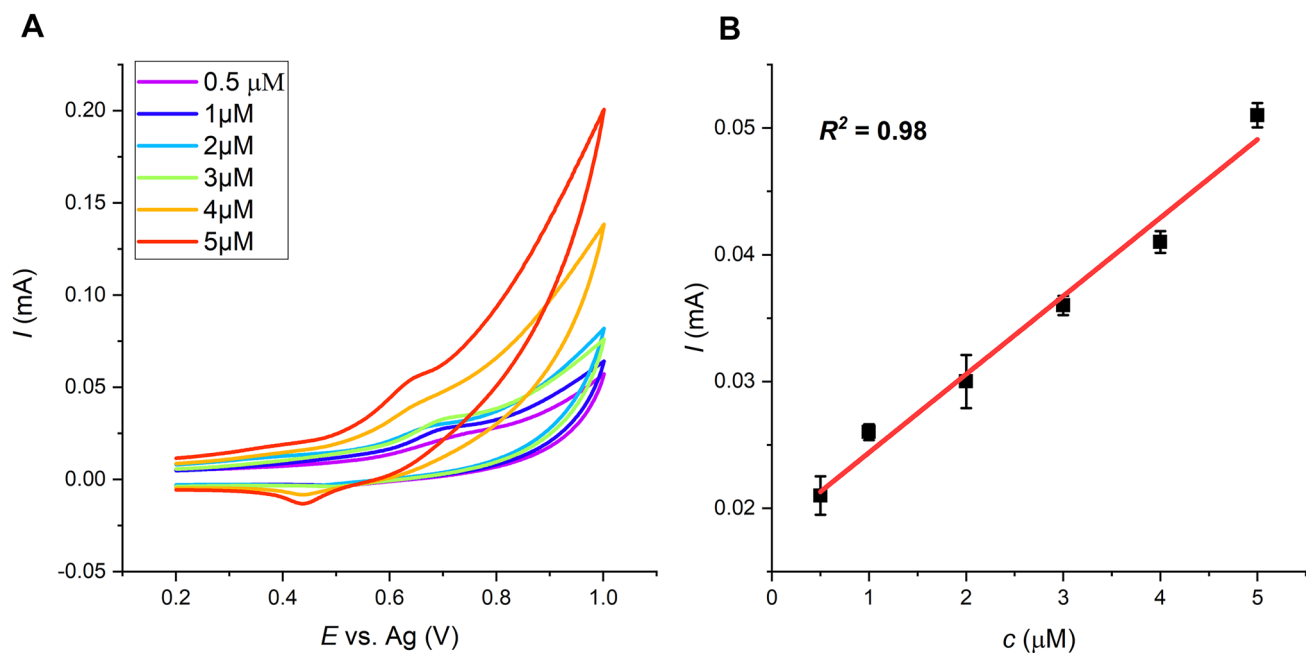


**Fig. 7** Cyclic voltammograms of various insulin concentrations (0.5–5  $\mu\text{M}$ ) on NiNPs-PPy-SPCE at a scan rate of 50 mV/s (A) in PBS with 0.1-M NaOH. The dependence of the maximal current value according to insulin oxidation on its concentration fitted by a linear function (B)



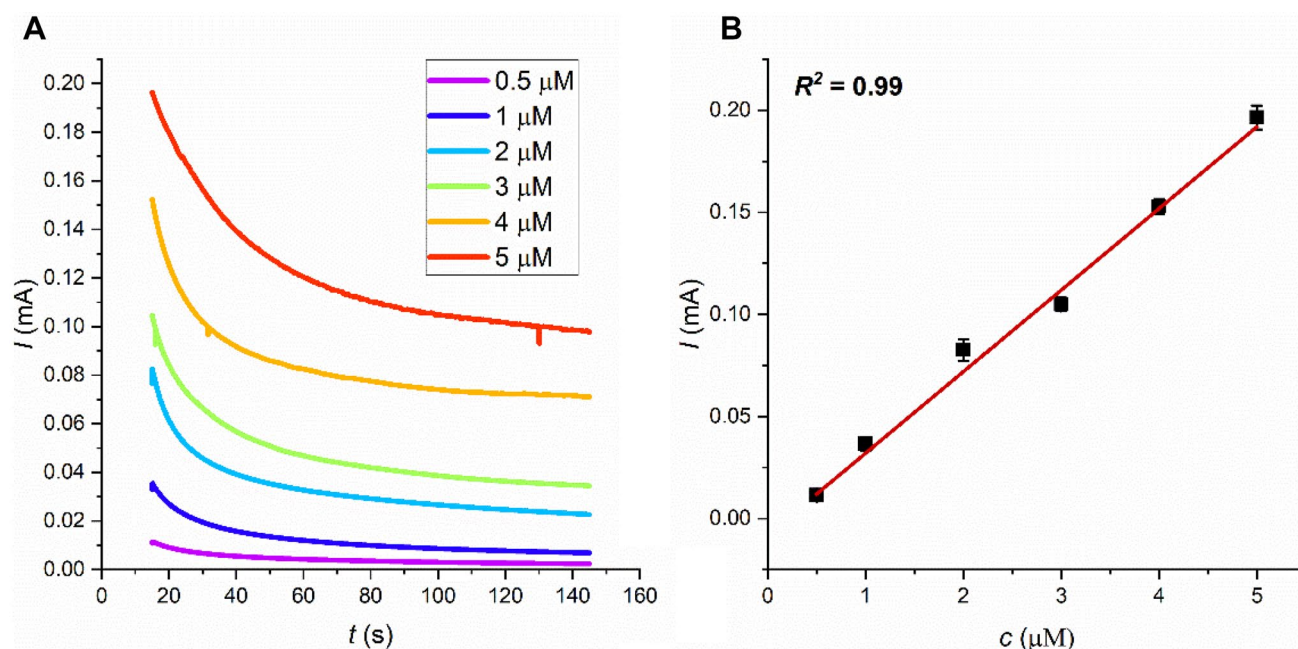


**Fig. 8** Chronoamperograms of different insulin concentrations on NiNPs-PPy-SPCE at potential  $E=0.62$  V in PBS with 0.1-m NaOH. The dependence of peak current on the insulin concentration, as fitted by a linear function (**B**)

measurement (Fig. 8). The results of chronoamperometry determination of insulin in the same concentration range (0.5 to 5  $\mu\text{M}$ ) were fitted by a linear function to calculate the sensing properties of the NiNPs-PPy-SPCE, as shown in Fig. 8B. NiNPs-PPy-SPCE displayed the same linear range from 0.5 to 5  $\mu\text{M}$  with  $R^2=0.99$ , with a LOD of 38 nM, calculated according to Eq. (4), and high sensitivity of 3.98  $\mu\text{A}/\mu\text{M}$ . The sensing properties of NiNPs-PPy-SPCE obtained by CV and CE were compared with other carbon electrode modifications published in international articles (Table 2). The modified electrode demonstrated sensing properties comparable to those of previously reported polymer electrode modifications, as the huge advantage of PPy usage as a conductive polymer can be considered increase of conductivity of prepared electrode in comparison with non-conductive polymer application, as was proved above in the text.

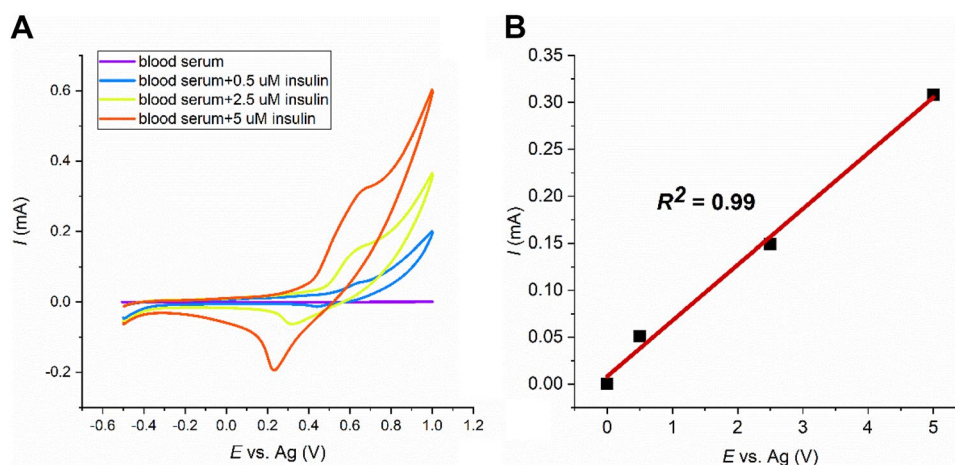
### Determination of Insulin in Blood Serum

To verify the reliability of the NiNPs-PPy-SPCE for routine analysis, commercially obtained human blood serum samples were used (Sigma Aldrich, Missouri). The presence of insulin can be declared by an oxidation peak at a potential of  $E=0.68$  V, which is approximately the same value as in PBS (Fig. 9). Moreover, the linear increase of peak current with the higher amount of insulin in the sample was observed (Fig. 9). These results were fitted by linear function (Fig. 9B) with correlation coefficient  $R^2=0.99$ , and the sensing properties of the NiNPs-PPy-SPCE in real samples were calculated according to Eq. (5). The calculated LOD was 44 nM, and the sensitivity was 5.96  $\mu\text{A}/\mu\text{M}$ . According to these results, NiNPs-PPy-SPCE can be considered a promising candidate for further clinical tests.

**Table 2** Electroanalytical parameters of different polymer-modified carbon electrodes used for insulin determination

Electrode	Linear range	Limit of detection	Sensitivity	Method	Ref
NiONPs/chitosan-MWCNTs/SPCE	0.25–5 $\mu\text{M}$	94 nM	0.02 $\mu\text{A}/\mu\text{M}$	Cyclic voltammetry	[47]
NiONPs/chitosan-MWCNTs/PGE	0.05–5 $\mu\text{M}$	85 nM	0.64 $\mu\text{A}/\mu\text{M}$	Cyclic voltammetry	[21]
CuNPs/chitosan-MWCNTs/SPCE	1–4 $\mu\text{M}$	1.11 $\mu\text{M}$	0.03 mA/ $\mu\text{M}$	Cyclic voltammetry	[8]
NiNPs-PPy-SPCE	0.5–5 $\mu\text{M}$	90 nM	6.65 $\mu\text{A}/\mu\text{M}$	Cyclic voltammetry	This work
NiNPs-PPy-SPCE	0.5–5 $\mu\text{M}$	38 nM	3.98 $\mu\text{A}/\mu\text{M}$	Chronoamperometry	This work

**Fig. 9** Cyclic voltammograms of different insulin concentrations on NiNPs-PPy-SPCE at a scan rate of 50 mV/s (A) in blood serum with 0.1-M NaOH. The dependence of peak current on the insulin concentration, as fitted by a linear function (B)



## Conclusion

In summary, application of two conductive polymer membranes (PANI and PPy) in development of non-enzymatic electrochemical sensors for insulin determination was studied and compared with non-conductive polymer (chitosan). The surface morphology of bare SPCE and modified SPCEs was studied via SEM and EDX analysis. Active surface area of all electrodes was determined electrochemically and calculated according to Randles-Ševčík equation. Based on obtained results, NiNPs-PPy-SPCE displayed the most suitable characteristics like the highest stability, conductivity, and the largest active surface area compared with bare electrodes and electrodes modified with other used polymers. Therefore, NiNPs-PPy-SPCE was used for various insulin concentration determinations in PBS and also in human blood serum. The prepared modified SPCE with combination of PPy and NiNPs exhibited favorable electroanalytical properties, like low LOD, high sensitivity, and stability. Furthermore, NiNPs-PPy-SPCE was able to detect insulin in real blood samples. In future work, we would like to realize the clinical study following multicentric clinical study to test NiNPs-PPy-SPCE in real clinical application.

**Acknowledgements** This research work has been supported by the project APVV-PP-COVID-20-0036 of the Slovak Research and Development Agency, by the Ministry of Education, Youth and Sports of the Czech Republic (DKRVO RP/CPS/2022/005), and by the Operational Program for Research, Development and Education, co-funded by the European Union within the framework of project No. CZ.02.2.69/0.0/0.0/18\_053/001/7879 entitled International Mobility of UTB Researchers in Zlín II.

**Author contributions** I.Š. - writing original draft, investigation, methodology. R.G. - visualization, writing - review and editing. F.CH. - data curation, investigation. J.S. - formal analysis. F.A.N. - data curation, writing - original draft. A.S.F. - validation. P.S. - supervising, conceptualization, funding. R.O. - writing - review and editing, supervising, funding.

**Funding** Open access funding provided by The Ministry of Education, Science, Research and Sport of the Slovak Republic in cooperation with Centre for Scientific and Technical Information of the Slovak Republic.

**Data and materials availability** Data available on request from the authors. The data that support the findings of this study are available from the corresponding author (RG) upon reasonable request.

## Declarations

**Ethical approval** Not applicable.

**Competing interests** The authors declare no competing interests.

**Open Access** This article is licensed under a Creative Commons Attribution 4.0 International License, which permits use, sharing, adaptation, distribution and reproduction in any medium or format, as long as you give appropriate credit to the original author(s) and the source, provide a link to the Creative Commons licence, and indicate if changes were made. The images or other third party material in this article are included in the article's Creative Commons licence, unless indicated otherwise in a credit line to the material. If material is not included in the article's Creative Commons licence and your intended use is not permitted by statutory regulation or exceeds the permitted use, you will need to obtain permission directly from the copyright holder. To view a copy of this licence, visit <http://creativecommons.org/licenses/by/4.0/>.

## References

1. M.M. Qaid, M.M. Abdelrahman, Cogent food agric. (2016). <https://doi.org/10.1080/23311932.2016.1267691>
2. M. Jaafariasl, E. Shams, M.K. Amini, Electrochim. Acta (2011). <https://doi.org/10.1016/j.electacta.2010.12.052>
3. G. Páth, N. Perakakis, C.S. Mantzoros, J. Seufert, Metabolism (2019). <https://doi.org/10.1016/j.metabol.2018.10.005>
4. I. Ahmed, B. Goldstein, Diabetes mellit. (2006). <https://doi.org/10.1016/j.clinidmatol.2006.04.009>
5. M. Pang, Y. Li, W. Gu, Z. Sun, Z. Wang, L. Li, Hear. Lung circ. (2021). <https://doi.org/10.1016/j.hlc.2020.07.015>
6. D.C. Simonson, Nephro-endocrinology (2009). <https://doi.org/10.1016/B978-0-12-373870-7.00025-9>

7. F. Gómez-Peralta, C. Abreu, X. Cos, and R. Gómez-Huelgas, "When does diabetes start? Early detection and intervention in type 2 diabetes mellitus," *Rev. Clínica Española* (English Ed., vol. 220, no. 5, pp. 305–314, (2020) <https://doi.org/10.1016/j.rceng.2019.12.004>.
8. I. Šišoláková, J. Hovancová, R. Oriňaková, A. Oriňak, L. Trnková, I. Třísková, Z. Farka, M. Pastucha, J. Radoňák, J. *Electroanal. Chem.* (2020) <https://doi.org/10.1016/j.jelechem.2020.113881>
9. I. Šišoláková, O. Petruš, J. Shepa, Z. Farka, A. Oriňak, R. Oriňaková, *Electroanalysis* (2021). <https://doi.org/10.1038/s41598-022-15283-7>
10. J. Hovancová, I. Šišoláková, P. Vanýsek, R. Oriňaková, I. Shepa, M. Kaňuchová, N. Király, M. Vojtko, P. Čudek, A. Oriňak, J. *Electroanal. Chem.* (2020). <https://doi.org/10.1016/j.jelechem.2020.114589>
11. S. Ammara, S. Shamaila, N. Zafar, A. Bokhari, A. Sabah, J. *Phys. Chem. Solids* (2018) <https://doi.org/10.1016/j.jpcs.2018.04.015>
12. N. Amini, M.B. Gholivand, M. Shamsipur, J. *Electroanal. Chem.* (2014). <https://doi.org/10.1016/j.jelechem.2013.12.015>
13. Y. Wang, X. Han, Z. Li, J. Xie, *Anal. Biochem.* (2019) <https://doi.org/10.1016/j.ab.2019.04.010>
14. M. Zhang, C. Mullens, W. Gorski, *Anal. Chem.* (2005). <https://doi.org/10.1021/ac0508752>
15. A. Noorbakhsh, A.I.K. Alnajjar, *Microchem. J.* (2016). <https://doi.org/10.1016/j.microc.2016.06.009>
16. P.K. Jiwanti, S. Sultana, W.P. Wicaksono, Y. Einaga, J. *Electroanal. Chem.* (2021). <https://doi.org/10.1016/j.jelechem.2021.115634>
17. G. Ibáñez-Redín, D. Wilson, D. Gonçalves, O.N. Oliveira, J. *Colloid interface sci.* (2018). <https://doi.org/10.1016/j.jcis.2017.12.085>
18. P. E. Resmi, J. Raveendran, P. V. Suneesh, T. Ramachandran, B. G. Nair, T. G. Sathesh Babu, *Mater. Lett.* (2021). <https://doi.org/10.1016/j.matlet.2021.130574>
19. A. Mahmoud, M. Echabaane, K. Omri, L. El Mir, R. Ben Chaabane, J. *Alloys compd.* (2019). <https://doi.org/10.1016/j.jallcom.2019.02.060>
20. E. Habibi, E. Omidinia, H. Heidari, M. Fazli, *Anal. Biochem.* (2016). <https://doi.org/10.1016/j.ab.2015.11.014>
21. I. Šišoláková, J. Hovancová, A. Oriňak, D.R. Garcia, O. Shylenko, J. Radoňák, *Electroanal.* (2018). <https://doi.org/10.1002/elan.201800483>
22. J. Shepa, I. Šišoláková, M. Vojtko, L. Trnková, G. Nagy, I. Maskaľová, A. Oriňak, R. Oriňaková, *Sensors* (2021). <https://doi.org/10.3390/s211155063>
23. D. Branagan, C. B. Breslin, *Sensors Actuators B. Chem.* (2019), 490–499, (2019). <https://doi.org/10.1016/j.snb.2018.11.089>
24. K.M. Ziadan, W.T. Saadon, *Energy procedia* (2012). <https://doi.org/10.1016/j.egypro.2012.05.184>
25. S. Sarkar, D. Das, P. Dutta, J. Kalita, S.B. Wann, P. Manna, *Carbohydr. Polym.* (2020). <https://doi.org/10.1016/j.carbpol.2020.116594>
26. N.K. Rawat, R. Ghosh, *Polymers* (2020). <https://doi.org/10.3390/polym8070249>
27. M.T. Ramesan, K. Suhailath, *Nanoparticle-based polymer composites*, 1st edn. (Elsevier Ltd., Netherlands, 2017), pp.124–130
28. G. De Alvarenga, J. *Electroanal. Chem.* (2020). <https://doi.org/10.1016/j.jelechem.2020.114754>
29. V.A. Online, S. Ahmad, *RSC Adv.* (2014). <https://doi.org/10.1039/C4RA06679K>
30. C. Emir, Y. Dilgin, A. Ramanaviciene, A. Ramanavicius, *Microchem. J.* (2021). <https://doi.org/10.1016/j.microc.2020.105751>
31. E. Nazarzadeh, *Appl. Mater. Today* (2021). <https://doi.org/10.1016/j.apmt.2021.101117>
32. J. Mostany, B.R. Scharifker, *Synth. Met.* (1997). [https://doi.org/10.1016/s0379-6779\(97\)80105-1](https://doi.org/10.1016/s0379-6779(97)80105-1)
33. Y. Li, R. Qian, *Electrochim. Acta* (2000). [https://doi.org/10.1016/S0013-4686\(99\)00392-8](https://doi.org/10.1016/S0013-4686(99)00392-8)
34. E. Lankinen, G. Sundholm, P. Talonen, T. Laitinen, T. Saario, J. *Electroanal. Chem.* (1998). [https://doi.org/10.1016/S0022-0728\(98\)00012-6](https://doi.org/10.1016/S0022-0728(98)00012-6)
35. A. Popov, B. Brasiunas, A. Damaskaite, L. Plikusiene, A. Ramanavicius, A. Ramanaviciene, *Polymers* (2020). <https://doi.org/10.3390/polym12122778>
36. M. Bazzaoui, J.I. Martins, S.C. Costa, E.A. Bazzaoui, T.C. Reis, L. Martins, *Electrochim. Acta* (2006). <https://doi.org/10.1016/j.electacta.2006.01.002>
37. S. Ding, *Biosens. Bioelectron.* (2020). <https://doi.org/10.1016/j.bios.2021.113434>
38. M. Chahma, C. Carruthers, *Sensors and actuators reports* (2021). <https://doi.org/10.1016/j.snr.2021.100039>
39. K. Cysewska, J.E. Soc, K. Cysewska, S. Virtanen, P. Jasi, J. *Electrochem. Soc.* (2015). <https://doi.org/10.1149/2.0821512>
40. A. Kisiel, D. Korol, A. Michalska, K. Maksymiuk, *Electrochim. Acta* (2021). <https://doi.org/10.1016/j.electacta.2021.138787>
41. M. Trchová, D. Jasenská, M. Bláha, J. Prokeš, J. Stejskal, *Spectrochim. Acta - Part A Mol. Biomol. Spectrosc.* (2020) <https://doi.org/10.1016/j.saa.2020.118300>
42. S.S. Bangade, V.M. Raut, S.E. Bhandarkar, D.P. Gulwade, *Mater. Today proc.* (2020). <https://doi.org/10.1016/j.matpr.2020.04.790>
43. J. Stejskal, J. Prokeš, *Synth. Met.* (2020). <https://doi.org/10.1016/j.synthmet.2020.116373>
44. N. German, A. Popov, A. Ramanaviciene, A. Ramanavicius, J. *Electrochem. Soc.* (2020). <https://doi.org/10.1149/1945-7111/abc9dc>
45. R. Devi, K. Tapadia, T. Maharana, *Heliyon* (2020). <https://doi.org/10.1016/j.heliyon.2019.e03122>
46. U. Samukaite-Bubiene, A. Valiuniene, V. Bucisnkas, P. Genys, V. Ratautite, A. Ramanaviciene, E. Aksun, A. Tereschenko, B. Zeybek, A. Ramanavicius, *Colloids Surf. A physicochem eng asp* (2020). <https://doi.org/10.1016/j.colsurfa.2020.125750>
47. I. Šišoláková, J. Shepa, L. Trnková, R. Oriňaková, A. Oriňak, *Bioelectrochemistry* (2019). <https://doi.org/10.1002/elan.201800483>

**Publisher's Note** Springer Nature remains neutral with regard to jurisdictional claims in published maps and institutional affiliations.